Proc. Natl. Acad. Sci. USA
Vol. 90, pp. 833–837, February 1993
Biochemistry

Twist and writhe of a DNA loop containing intrinsic bends

WILLIAM R. BAUER*, RUSSELL A. LUND†, AND JAMES H. WHITE†

*Department of Microbiology, School of Medicine, State University of New York, Stony Brook, NY 11794-5222; and †Department of Mathematics, University of California at Los Angeles, CA 90024-1555

Communicated by Peter H. von Hippel, October 12, 1992

ABSTRACT **The finite-element method of solid mechanics is applied to calculation of the three-dimensional structure of closed circular DNA, modeled as an elastic rod subject to large motions. The results predict the minimum elastic energy conformation of a closed loop of DNA as a function of relaxed equilibrium configuration and linking number (Lk). We apply the method to four different starting states: a straight rod, two rods containing either one or two 20° bends, and a circular O-ring. The results, here at low superhelix density, show the changes in writhe (Wr) and in twist (Tw) as Lk is progressively lowered. The presence of even a single intrinsic bend reduces significantly the linking number change at which Wr first appears, compared to an initially straight, bend-free rod. The presence of two in-phase bends, situated at opposite ends of a diameter, leads to the formation of at least two distinct regions of different but relatively uniform Tw increment. The O-ring begins to writhe immediately upon reduction of Lk, and the Tw increment distribution is sinusoidal along the rod. The mechanics calculations, unlike other theoretical approaches, permit us to calculate Tw and Wr independent of the constraint of constant Lk.**

The three-dimensional structure of closed circular DNA has been much studied, both experimentally and theoretically, but a coherent picture is only beginning to emerge. From the theoretical point of view, the first requirement is specification of a model to represent the DNA at the desired level of complexity. It has long been clear that many of the tertiary structural properties of DNA in general, and of closed DNA in particular, may be represented by an elastic isotropic rod of circular cross section (1), or a wormlike chain (2). The rod is subject to bending, torsional, and extension distortions and possessed of the corresponding three structural moduli (3). This is the model that is commonly used to represent DNA for didactic purposes, and the object of the present study is to determine theoretically what are the equilibrium conformations of such a closed circular DNA at various imposed deformations.

For analytical purposes, it is convenient to divide the calculations into two regions. At very low linking-number changes (ΔLk), the deformations of the DNA are moderate and distal parts of the molecule remain separated. At moderate to high ΔLk, however, distant chain segments are brought into proximity and the problem of forbidden self-passage arises. We will treat only the first case, that of low ΔLk, in the present article; the problems associated with self-passage will be treated elsewhere. This case is of importance in its own right, since it allows us to deal with the looping of segments of a long, linear DNA, in which closed circular topological domains of low ΔLk are formed (4, 5).

It is well known that a closed circular DNA has a linking number, Lk, and that this topological property subdivides into the two geometric properties (6, 7): twist, Tw (duplex distortion), and writhe, Wr (axis distortion). We analyze how a small ΔLk applied to a closed circular DNA is distributed between Tw and Wr. Four classes of DNA are considered. Two are the extreme cases: first, a DNA that is strain-free as a linear molecule, then bent smoothly to form a strained circle; second, a DNA that is naturally strain-free in the circular form. The first case is represented by a straight elastic rod, and the second by an O-ring. Representations of these in their strain-free states are shown in Fig. 1, which also defines the terminology used to describe the structures. The O-ring is the limiting case produced by a continuous, in-phase sequence of identical intrinsic bends. Short DNA molecules having an O-ring structure have been synthesized (8). Intrinsically bent regions are found in DNA (9, 10), as are bends induced by protein binding (11), and one of our major objectives is to determine the effect of bends on the structure of circular DNA. We therefore analyze two cases in which the DNA contains either one or two intrinsic bends: an elastic rod with one 20° bend, and an elastic rod with two in-phase 20° bends. In-phase means that the bends lie in the same plane and are oriented the same with respect to the interior of the loop. In order to represent a closed DNA, all models that are initially open are first closed, producing shapes shown in Fig. 2.

We find that the distribution of ΔLk between Tw and Wr varies markedly among the four cases. For the initially straight rod, a considerable change in ΔLk is required to introduce Wr. In addition, the change in Tw is seen to be uniformly distributed along the length of the rod. The presence of a single intrinsic bend is seen to convert a portion of Tw immediately into Wr, but the remaining Tw is still divided uniformly. The addition of a second intrinsic bend, in-phase and diametrically opposite, results in only a small change in the point at which Tw is converted into Wr. The Tw increment distribution, however, is strikingly altered: the Tw is no longer uniform but is discontinuous at the bend locations. Finally, in the O-ring case a large portion of ΔLk is converted into Wr, and the Tw increment is sinusoidally distributed along the O-ring axis. In summary, bent DNA converts Tw into Wr much more efficiently than unbent DNA, and the presence of bends causes nonuniformities in the local Tw increment. Both of these features may well have significant structural consequences for interpreting the biological effects of looping and of other phenomena involving the three-dimensional structure of DNA.

THEORY AND MODELS

We model the DNA as a linearly elastic rod having the appropriate cross section and material moduli, including the modulus of elasticity and the shear modulus. The cross section is taken to be circular of radius 1 nm, for which the moment of inertia, I, is equal to $\pi/4$ nm^4. The modulus of elasticity, E, is estimated from the persistence length, λ, with the expression $E = \lambda k_B T/I$, where k_B is the Boltzmann constant and T the temperature (298 K). For a DNA persistence length (at moderate ionic strength) of 200 bp (3, 12) the

The publication costs of this article were defrayed in part by page charge payment. This article must therefore be hereby marked "*advertisement*" in accordance with 18 U.S.C. §1734 solely to indicate this fact.

Abbreviations: Lk, linking number; Tw, twist; Wr, writhe; FEM, finite-element method.

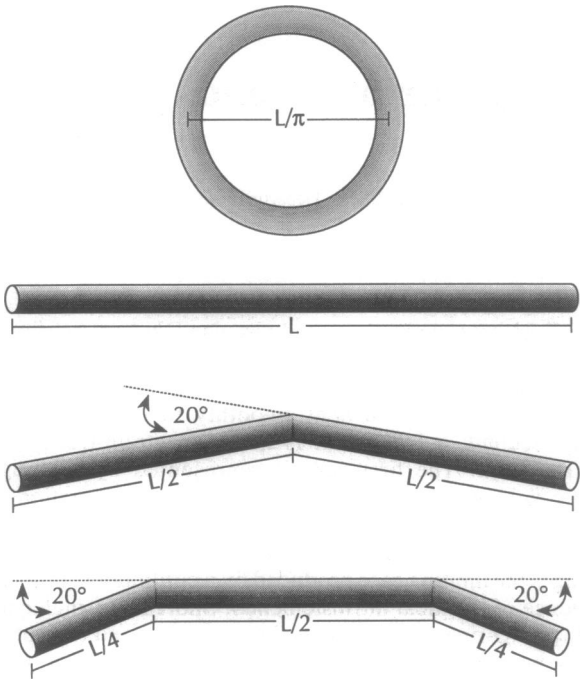

FIG. 1. Models for classes of strain-free DNA. Four initial configurations with no internal strain energy are shown: O-ring, straight linear, linear with single 20° bend, and linear with two in-phase 20° bends separated by one-half the length of the rod. The length of each model, L, is 2100 bp in the calculations performed here.

value of E is 3.40×10^9 dyne·cm^{-2}. The shear modulus, G, is obtained from the torsional rigidity, C, with the expression $G = C/2I$. For the value of $C = 2.5 \times 10^{-19}$ erg·cm (13, 14), the value of G is 1.59×10^9 dyne·cm^{-2}. The calculations are performed for a DNA of length 630 nm, or 2100 bp, about half the length of pBR322 DNA (4361 bp).

To apply the elastic rod model to closed circular DNA, we must specify how to introduce changes in ΔLk. The three classes of DNA that are straight, singly bent, and doubly bent in their strain-free form must first be closed (Fig. 2). The O-ring model is already closed in its strain-free state. Each rod is then cut perpendicular to its axis. The two faces of this cut are next caused to rotate relative to one another about the local tangent to the rod axis and then resealed. This process has the effect of changing ΔLk fractionally by the amount of rotation imposed.

In response to the imposed change in boundary conditions, as represented by a change in ΔLk, the various rod models undergo deformation. The problem is to calculate the new coordinates of each rod—i.e., its new shape. This is accomplished by the methods of solid mechanics. Solid-mechanics principles give rise to nonlinear continuous differential equations with boundary conditions. Solid mechanics includes the requirement of mechanical equilibrium (balance of forces), in addition to the constitutive relationships such as Hooke's Law. At stable equilibrium, the total potential energy of an elastic structure is locally minimum. The coordinates that describe each rod following cut, rotation, and resealing are obtained from the newly calculated displacement field, which consists of the vectors joining points on the initial configuration to their corresponding points on the new configuration. Solution of the equations to obtain the displacement field requires, due to their complexity, numerical techniques such as provided by the finite-element method (FEM).

NUMERICAL MODELS AND METHODS

Displacement-based FEM is a powerful and well-established technique for obtaining solutions to problems in nonlinear

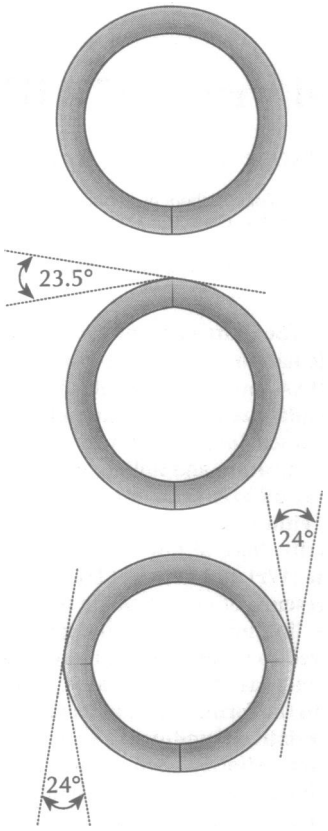

FIG. 2. Models for classes of closed DNA. The structures shown here were obtained from the three open forms shown in Fig. 1 by closing each rod in the x–z plane. Closure was accomplished by gradually moving one end of the rod relative to the other and enforcing equilibrium throughout the process. The bend angle increases to 23.5° in the singly bent rod and to 24.0° in the doubly bent rod.

solid mechanics. Numerous displacement-based finite-element programs have been written, and many are available commercially. The initial configurations are modeled, in the FEM context, as three-dimensional continua. The DNA rod is divided along its axis into a discrete number of appropriately curved segments, here taken to be 40. Each of these curved cylindrical segments is further subdivided into four equal quadratic elements (Fig. 3) in order to capture the geometry of the initial configuration. The four elements join at the centroid of the rod, and each element is described by 20 nodal points. This division produces 160 finite elements and 1221 distinct nodal points. The DNA rod is constituted of linear elastic material with E, G, and cross-sectional radius as given above.

In displacement-based FEM the fundamental variables are the displacements (15). The continuous displacement vector field is approximated by a collection of individual element displacement fields that depend on values of displacements at the nodal points. In the present work the components of the individual element displacement fields are given by quadratic interpolation functions. Displacements are continuous across interelement boundaries, and no restriction is placed on the displacement magnitudes. After imposing displacement boundary conditions, the models have ≈3500 displacement degrees of freedom (independent variables). The number of elements per DNA is varied to pick conditions for which the results are relatively insensitive to the element size and for which the choice of quadratic interpolation functions is adequate for both the geometry and the nodal displacements.

In solving nonlinear problems with FEM, one effective approach is to apply the boundary conditions incrementally.

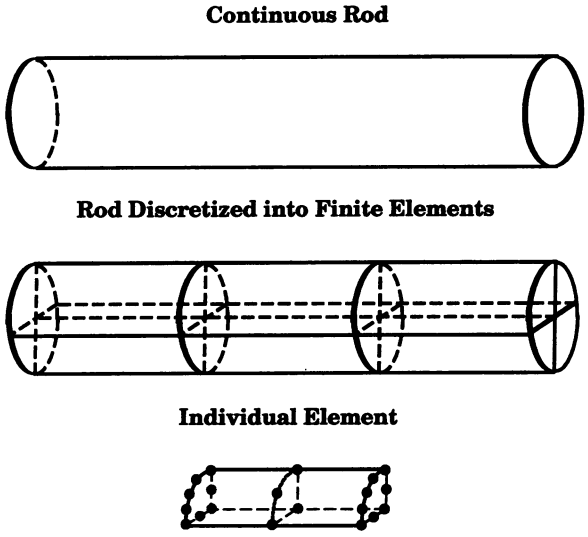

FIG. 3. Choice of finite elements for an elastic rod. The case depicted is that of the straight rod, which is here divided into three discrete sections. Each section is divided into four equal parts, as shown. It is these quadrants that form the finite elements. Twenty nodal points, shown as filled circles on the element sketch, are used for two purposes: to define individual element geometry and to determine the quadratic element-displacement field parameters. In the analysis presented here, each DNA rod is divided into 40 sections, and therefore into 160 finite elements.

The nonlinear equations may then be solved by a sequence of linear approximations to the governing relations. This is accomplished by eliminating higher-order terms in the displacement increments. In each increment an iterative procedure is used to correct for the errors introduced by linearization.

Solutions reported here were obtained by using the MARC computer program (16), a well-known general-purpose displacement-based finite-element code with both linear and nonlinear capabilities. The updated Lagrangian formulation was used to treat large displacements. Several benchmark problems were analyzed to verify program capabilities. The program was run on an IBM 3090 model J computer. Convergence criteria internal to the MARC program include a measure of the equilibrium error and the maximum displacement during an iteration. In addition to these criteria, iteration convergence was assessed by consideration of change in conformation as measured by Wr, a measure in this case of the out-of-plane motion of the axis of the rod. Three or four iterations were typically required for suitable convergence; for situations of substantial motion with applied rotation increment as many as 12 iterations were required. Typical increments used 80–90 sec of central-processing-unit time.

RESULTS

Geometry. Each of the closed configurations was subjected to relative rotation (change in Lk) up to the point at which initially remote segments of the model begin to come into contact. Fig. 4 shows examples of each of the four cases, chosen so that Wr ≈ -0.03 for all. Three views are depicted for each, in order to illustrate various geometric properties. The view along the y axis clearly distinguishes the three models. The elliptical shape characterizes the initially straight model and contrasts markedly with the egg shape introduced by the single bend. In the double-bend model, the two flattened portions of the curve indicate the locations of the bends. The flattened region in the O-ring corresponds to the location of the cut. The view along the x axis indicates the maximum in the projected Wr and best shows the distortion in each.

Wr. Fig. 5 presents a plot of Wr as a function of total relative rotation for each model. The initially straight configuration, which forms a circular shape upon closure, is capable of sustaining a relatively large amount of rotation prior to the onset of measurable writhe. No Wr is observed to occur until the relative rotation reaches about -1.80 turns (Fig. 5*B*). This is in good agreement with other analyses in the literature, which predict the onset of Wr at $-\sqrt{3}(E/2G) = -1.85$ turns (17, 18). The O-ring configuration, in contrast, begins to writhe immediately upon imposition of relative rotation to change ΔLk.

The two initially bent configurations behave intermediate between that of the rod and of the O-ring. The results show that a change in ΔLk in either causes deformation by an amount intermediate between the two extreme models. Even the singly bent molecule begins to writhe directly upon application of rotation, a feature more in common with the O-ring than with the linear rod. The point at which Tw is rapidly converted to Wr occurs at a significantly lower applied rotation than for the initially straight model. The

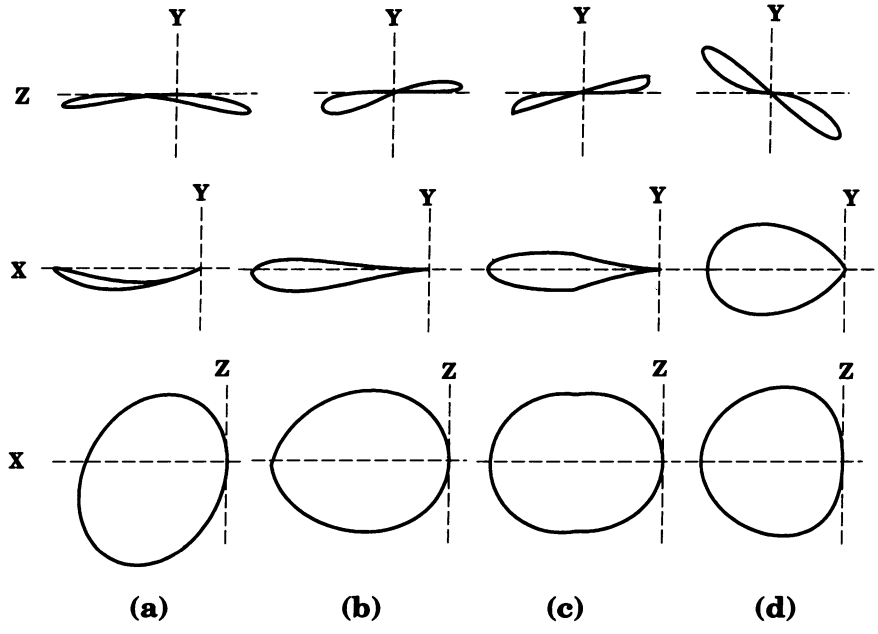

FIG. 4. Representative closed DNA structures, having similar Wr, at various applied rotations. (*a*) Initially straight, rotation of 2.075 turns. (*b*) Single bend, 1.625 turns. (*c*) Double bend, 1.50 turns. (*d*) O-ring (initially circular), 0.375 turn. For each configuration, three projected views are shown: proceeding from top to bottom these are along the x, z, and y axes, respectively.

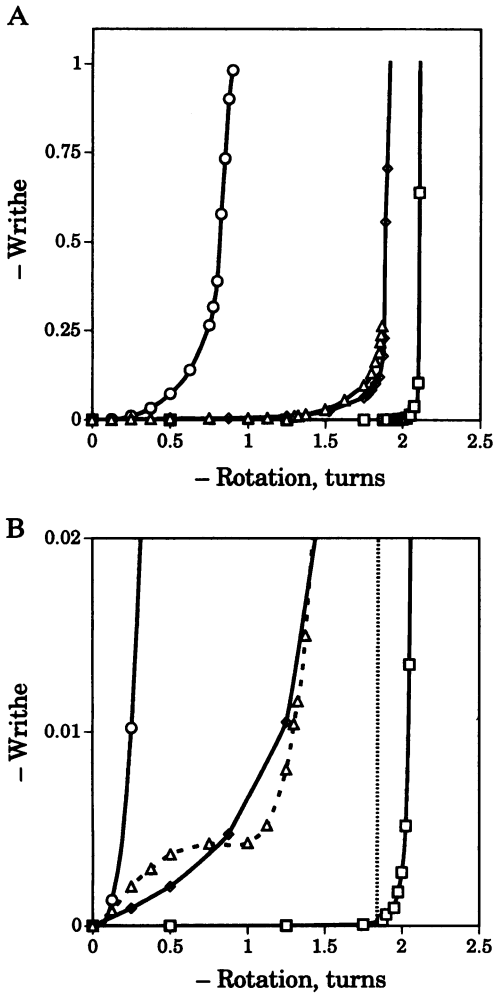

FIG. 5. Variation of Wr with ΔLk (applied rotation). In *A* the results are shown over the range 0 to −1 in Wr. *B*, at an ≈50-fold magnified scale, shows that both bent molecules begin to writhe immediately upon even a very small applied rotation. This is in contrast to the initial straight rod, in which the onset of Wr is considerably delayed. The behavior of the double-bend curve in the region between 0.75 and 1.25 turns is possibly caused by the fact that closure of this structure resulted in a slight relative out-of-plane motion of the bends. The curves refer to the various models as follows: □, initially straight rod; ◇, singly bent rod; △, doubly bent rod; and ○, O-ring. The vertical dotted line in *B* represents the linear elasticity theoretical threshold for the onset of Wr (17, 18).

behavior of the molecule containing two identical bends, diametrically opposite and in phase, is generally similar to the singly bent DNA. We expect the conversion of Tw into Wr to depend upon the magnitude and relative orientation and location of the bends; this will require further investigation. The FEM analysis of the continuous model of closed DNA clearly predicts that even a single intrinsic bend can have a large effect upon the three-dimensional structure of a looped DNA.

Tw. An important facet of the present work is the ability to compute directly ΔTw from the initial configuration to the final configuration. Tw is defined to be the twist of a backbone chain, B, about the central axis, A. The backbone curve may be thought of as a helical curve winding about the axis on the surface of the elastic rod. If the rod models in Fig. 2 are made to rest on the surface of a plane, we may define a curve C as the curve of contact of each model with the plane. Each of these is a closed curve that traverses the length of the rod. The axis of the rod is then the curve of height 1 nm above the curve C. One may show, using the method of twist difference analysis (19), that the change in Tw of B about A is the same as that of C about A. For the initial configuration the Tw of C about A is clearly zero. Thus, ΔTw is given by the Tw of the deformed C about the deformed A. This can be computed by using the correspondence techniques described by us previously (20). ΔTw is computed piecewise by dividing each of the 40 curved elements into two straight segments. Because Tw is an additive function, the total Tw is given by the sum of these 80 incremental Tw values.

In addition to the total ΔTw, the distribution of ΔTw along each DNA rod is strongly influenced by the nature of the initial, strain-free configuration. For the initially straight model ΔTw is distributed uniformly along the length of the DNA (Fig. 6). For the O-ring, ΔTw varies sinusoidally along the rod with maximum and minimum absolute values at diametrically opposite locations. For the singly bent DNA, as for the initially straight model, ΔTw remains uniform. For the doubly bent model, however, ΔTw is nonuniform. The addition of a second bend into the DNA divides the DNA into two regions of relatively uniform Tw, with each bend causing a discontinuity in the twist. The ΔTw distributions in Fig. 6 are plotted with reference to the location of the cut, which is taken to be the origin. Tw distributions are fixed relative to the cut location by FEM boundary conditions. Since thermal fluctuations are not modeled, the results are effectively at 0 K. If the temperature of the initially straight or O-ring DNA were reversibly increased and the molecules incubated at (say) room temperature, then reversibly decreased again to 0 K, the shape of the Tw increment distributions would be unchanged but would be shifted randomly relative to each cut location.

DISCUSSION

The FEM-based calculations yield the DNA structure of minimum elastic energy at 0 K. The energy involved is one of the two components of the Helmholtz free energy (work function), and at constant DNA length is identical to the

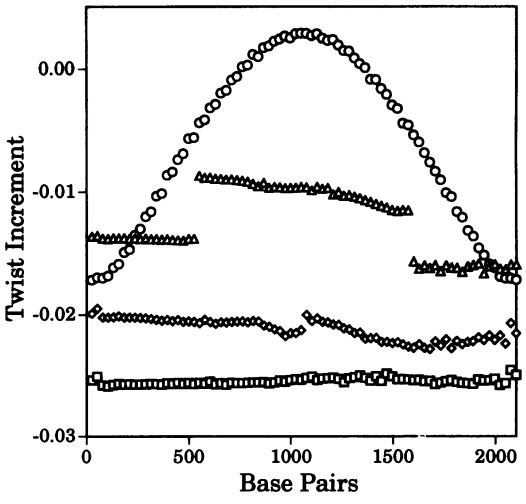

FIG. 6. Variation of the Tw increment as a function of distance along the DNA for a particular ΔLk for representative examples of the various models. The initially straight and the singly bent rods exhibit uniform Tw. The doubly bent rod shows regions of relatively uniform Tw separated by discontinuities. The O-ring shows sinusoidal variation in Tw along its length. The total ΔTw, Wr, and applied rotation for each are as follows: straight rod (□), ΔTw = −2.038, Wr = −0.037, ΔLk = −2.075; singly bent rod (◇), ΔTw = −1.695, Wr = −0.179, ΔLk = −1.875; doubly bent rod (△), ΔTw = −0.994, Wr = −0.004, ΔLk = −1.000; O-ring (○), ΔTw = −0.483, Wr = −0.265, ΔLk = −0.750.

enthalpy of superhelix formation. Previous theoretical examinations of the structure of closed DNA have employed either small displacement elastic models or stochastic calculations. In the former studies, linear approximations were used to estimate the elastic response of small DNAs (21–24). Stochastic approaches have employed either Monte Carlo simulations or annealing by molecular dynamics. Monte Carlo methods have been used to describe the expected variance in Wr (25, 27) and in the equilibrium configuration (28). They represent a compromise, in which bending occurs at finite temperatures but Tw is assumed to be uniform, as expected for an initially straight rod, excluding thermal fluctuations. The molecular dynamics calculations attempt to follow the contortions of a single molecule through time at finite temperature. They would, in principle, be complete if applied to a real molecular model of the DNA. Since this is prohibited by the complexity of the atomic structure, the procedures of molecular mechanics and dynamics have been applied to models that are highly simplified in structure. Examples include three points in connected planes (29) and discrete points joined by B spline curves (30). In principle, both the Monte Carlo and the molecular dynamics methods allow for the calculation of the free energy.

In contrast to the above methods, application of solid mechanics via the finite-element method avoids the use of stochastic methods and of small displacement approximations. FEM predicts conformations for particular prescribed loadings. Instead of sampling configuration space, the calculations are deterministic. Thus, for example, FEM provides specific equilibrium conformations as a function of ΔLk for closed molecules, whereas the Monte Carlo techniques yield a large number of conformations at a given ΔLk. The various conformations are considered to vary about the equilibrium shape, with variations attributed to thermal fluctuations. While FEM analysis can be numerically intensive, the number of calculations is finite for a given level of accuracy. The stochastic methods, however, must be repeated for a sufficiently large number of trial conformations to obtain a reliable estimate of the average conformation. Elastic properties are directly incorporated in the FEM solution, in contrast with rigid-link Monte Carlo methods, for which restrictions are placed on possible values of discrete angles between adjoining segments of the model. These latter restrictions are intended to reflect internal energy minimization principles but do not require satisfaction of mechanical equilibrium for individual conformations.

Previous investigations used models for which Tw is uniform along the DNA, although an approximation to Tw was computed in one study (29). In the Monte Carlo, spline, and molecular dynamics techniques, this assumption is necessary because ΔTw is obtained from the relationship: Tw = Lk − Wr. In general, the stochastic methods are not well suited to calculate local ΔTw within a DNA molecule. The FEM calculations show, in contrast, that the local Tw can vary significantly and that this variation is sensitive to the presence of intrinsic bends.

The closure of DNA rods into circles or loops is increasingly recognized to be an important mechanism in the regulation of certain metabolic pathways (4). In this process the DNA segment forms a topological domain that may contain bends, either intrinsic or protein-induced (31). The formation of a loop generally occurs with only a small amount of net interstrand rotation (e.g., to permit alignment of protein faces); hence, the results obtained by us are relevant to understanding the geometry and energetics of loop formation. Thus, a DNA loop containing a bend is expected to writhe, as the ends are rotated, before the same loop without a bend. The presence of two bends might produce a region of greater than average strain (as shown by the increased Tw increments). This might, in turn, influence the binding of proteins or other aspects of reactivity.

This research was supported in part by Grant GM37525 from the National Institutes of Health. Computer support was supplied by the Office of Academic Computing at the University of California, Los Angeles.

1. Landau, L. D. & Lifschitz, E. M. (1958) *Statistical Physics* (Addison–Wesley, Reading, MA).
2. Kratky, O. & Porod, G. (1949) *Recl. Trav. Chim. Pays-Bas* **69**, 1106–1122.
3. Manning, G. S. (1988) *Biopolymers* **27**, 1529–1542.
4. Schleif, R. (1988) *Science* **240**, 127–128.
5. Lobell, R. B. & Schleif, R. F. (1990) *Science* **250**, 528–532.
6. White, J. H. (1989) in *Mathematical Methods for DNA Sequences*, ed. Waterman, M. S. (CRC, Boca Raton, FL), pp. 225–253.
7. White, J. H. (1969) *Am. J. Math.* **91**, 693–728.
8. Ulanovsky, L., Bodner, M., Trifonov, E. N. & Choder, M. (1986) *Proc. Natl. Acad. Sci. USA* **83**, 862–866.
9. Marini, J. C., Levene, S. D., Crothers, D. M. & Englund, P. T. (1982) *Proc. Natl. Acad. Sci. USA* **79**, 7664–7668.
10. Wu, H. M. & Crothers, D. M. (1984) *Nature (London)* **308**, 509–513.
11. Travers, A. A. (1989) *Annu. Rev. Biochem.* **58**, 427–452.
12. Barkley, M. D. & Zimm, B. H. (1979) *J. Chem. Phys.* **70**, 2991–3007.
13. Horowitz, D. S. & Wang, J. C. (1984) *J. Mol. Biol.* **173**, 75–91.
14. Shore, D. & Baldwin, R. L. (1983) *J. Mol. Biol.* **170**, 957–981.
15. Bathe, K.-J. (1982) *Finite Elements in Engineering Analysis* (Prentice–Hall, Englewood Cliffs, NJ).
16. MARC (1983) *General Purpose Finite Element Program, Vol. A* (MARC Analysis Res. Corp., Palo Alto, CA).
17. Benham, C. J. (1989) *Phys. Rev. A* **39**, 2582–2586.
18. Le Bret, M. (1979) *Biopolymers* **18**, 1709–1725.
19. White, J. H. & Bauer, W. R. (1988) *Proc. Natl. Acad. Sci. USA* **85**, 772–776.
20. White, J. H. & Bauer, W. R. (1986) *J. Mol. Biol.* **189**, 329–341.
21. Shimada, J. & Yamakawa, H. (1985) *J. Mol. Biol.* **184**, 319–329.
22. Benham, C. J. (1983) *Biopolymers* **22**, 2477–2495.
23. Hunt, N. G. & Hearst, J. E. (1991) *J. Chem. Phys.* **95**, 9329–9336.
24. Schlick, T. & Olson, W. K. (1992) *J. Mol. Biol.* **223**, 1089–1119.
25. Klenin, K. V., Vologodskii, A. V., Anshelevich, V. V., Klishko, V. Y., Dykhne, A. M. & Frank-Kamenetskii, M. D. (1989) *J. Biomol. Struct. Dyn.* **6**, 707–714.
26. Chen, Y.-D. (1981) *J. Chem. Phys.* **75**, 2447–2453.
27. Shimada, J. & Yamakawa, H. (1988) *Biopolymers* **27**, 657–673.
28. Hao, M.-H. & Olson, W. K. (1989) *Macromolecules* **22**, 3292–3303.
29. Tan, R. K. Z. & Harvey, S. C. (1989) *J. Mol. Biol.* **205**, 573–591.
30. Hao, M. H. & Olson, W. K. (1989) *J. Biomol. Struct. Dyn.* **7**, 661–692.
31. Lobell, R. B. & Schleif, R. F. (1991) *J. Mol. Biol.* **218**, 45–54.